Journal of Petroleum Research and Studies

Open Access
No. 40, September 2023, pp. 59-73

P- ISSN: 2220-5381
E- ISSN: 2710-1096

DOI: http://doi.org/10.52716/jprs.v13i3.704

Detection of Over Normal Pore Pressure Intervals by Using Well Logs

Jassim M. Al Said Naji[1*], Ghassan H. Abdul-Majeed[2], Ali K. Alhuraishawy[3], Ameer Talib[4]

[1]University of Technology, Baghdad, Iraq

[2]University of Baghdad, Baghdad, Iraq

[3]Ministry of Oil, Baghdad, Iraq

[4]Petroleum Research and Development Center, Baghdad, Iraq.

[1*]Corresponding Author E-mail: 150100@uotechnology.edu.iq.

[2]ghassan@uob.edu.iq.[3]ali19_82@yahoo.com.[4]optimism92@yahoo.com.

Received 12/10/2022, Revised 05/11/2022, Accepted 10/11/2023, Published 10/09/2023

Abstract

Pore pressure is very important parameter that impacting on drilling, production planning and operations. Drilling and production processes cannot be beginning if pore pressure is not estimated. There is a limit of difference between hydrostatic pressure of mud column and pore pressure during drilling to ensure that the layers are preserved from fracturing, as well as that kicking does not occur inside the well. Difference between pore pressure and bottom hole flowing pressure is a key for production process. Over (Abnormal) pressure intervals are causing many problems during drilling. In present study, pore pressure is estimated firstly as a hydrostatic pressure, and secondly, after determination of shale flag, two methods of Eaton slowness and Bowers original are used for detecting of over (Abnormal) pressure shale intervals. Compressional and density logs of three wells (X3, X4, and XD) located at Y oil field and producing from Asmari formation are used to perform the present study. Density log is linearly extrapolated to estimate bulk density from zero depth to last depth point at reservoir. Vertical stress is predicted for these three wells. The vertical stress gradients were 1.03, 0.99, and 0.93 psi/ft for XD, X3, and X4 wells respectively. Results are reveals that Bowers original better than Eaton slowness in detection of over (abnormal) pressure intervals where the last did not cut all shale intervals by compressional slowness shale base line that equal to 80 us/ft so, Eaton slowness method provided either very high over pressure in some shale intervals or subnormal pressure to other shale intervals and that inaccurate while Bowers original method approximately provided all shale intervals as over pressure in reasonable values. Modular dynamic tester measurements for pore pressure of these three wells are used for calibration. Maximum percent error between predicted and measured pore pressure of wells (X3, X4, and XD) are 1.2%, 0.89% and 3% respectively where these percent are very acceptable. Maximum over pressure values in

Open Access
No. 40, September 2023, pp. 59-73

P- ISSN: 2220-5381
E- ISSN: 2710-1096

Asmari formation zones at wells are as follows: 6328 psi at depth 3225 m in well X3, 7538 psi at depth 3080 m in well X4, and 6731 psi at true vertical depth 3067 m in well XD.

Keywords: Pore pressure, Vertical stress, Shale flag, Bowers original, Eaton slowness.

1. Introduction:

Pore pressure (P_p) and fracture gradient determination are key components of the exploration, drilling, and well completion planning processes in diverse and complicated geological settings [1]. Fluids that filled the pore space put pressure on the pore wall, which results as P_p. [2]. P_p estimation is based on Terzaghi principle and Biot law, where they are dealt with estimation of effective stress according to determined P_p, as well as, they accounted source of up-normal (over and under) pressure as disequilibrium compaction criteria [3]. Accurate P_p prediction need to determine its relation with reservoir properties, evaluating of seals and analyzing subsurface hydrodynamic system for hydrocarbon migration pattern [4], i. e. porosity and permeability with both elastic and strengths components decrease when P_p decreases and effective confining pressure increases. Additionally, if the P_p drop is large enough, the resulting increase in effective stress might lead to an irreversible loss of strength, resulting in plastic deformation [5]. P_p holds a portion of S_v, whereas rock grains hold the remainder. Depend on the P_p value; it classified into three types as illustrated in **Figure (1).**

Normal Pore pressure (P_{norm}) corresponds to the formation pore pressure exerted by fluid column ranging from the surface to the depth of interest. The usual P_{norm} gradient is about 0.465 psi/ft for saltwater and 0.433 psi/ft for fresh water. It is depending on density of water where density related with salinity, dissolved gas, and temperature. P_{norm} gradient (0.465 psi/ft) equivalent to 80000 ppm water salinity [6]. This gradient stated by [7] as 0.1 – 0.2 psi/ft for gas and 0.25 – 0.4 psi/ft for oil.

Over-normal (Abnormal) pore pressure is a pore pressure greater than P_{norm}. many mechanisms can produce overpressures, including compaction disequilibrium, hydrocarbon generation and gas cracking, aqua-thermal expansion, tectonic compression (lateral stress), mineral transformations (e.g., illitization), and osmosis, hydraulic head, shale existing and hydrocarbon buoyancy [8, 9]. Generally, abnormal pressure gradient ranges between 0.8 and 1 psi/ft [10].

Sub-normal Pore Pressure is a pore pressure lower than normal pressure at a given depth [11]. Subnormal formation pressures can be developed explicitly by extracting oil, gas, and/or

Open Access
No. 40, September 2023, pp. 59-73

P- ISSN: 2220-5381
E- ISSN: 2710-1096

water from permeable reservoirs. The production of high volumes of reservoir fluids can significantly decrease formation pressure [12, 13].

Aim of present paper is detection of over pressure intervals for three wells penetrated Asmari formation of Y oil field by using well logs data.

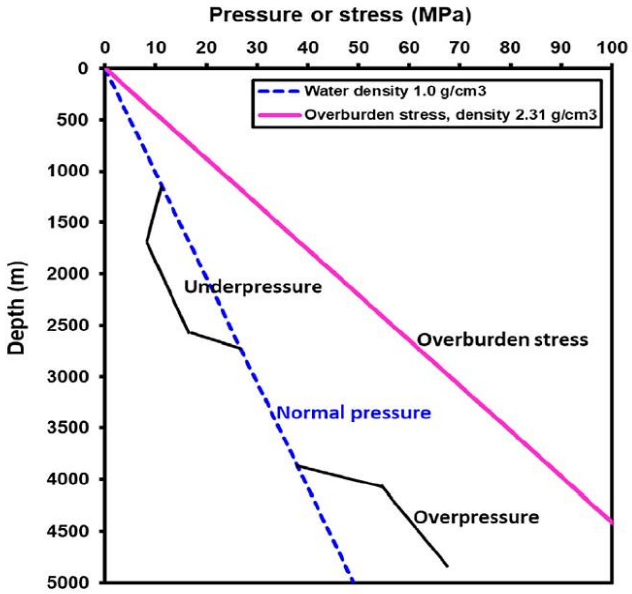

Fig. (1): Pore pressure types [14].

1.1. Field and Formation of Study

Y oil field is one of the southern Iraqi oil fields that located in Missan governorate, far of 175 km north of Basrah city and 50 km to north–east of Ammara city A few kilometers than Buzrgan oil field. It is existing near Iraqi Irainian borders and some of its parts locate in Iran as shown in **Figure (2)**. It has two north and south domes and feed from two formations Asmari and Mishrif. Asmari is a formation of study. It has width about 23 km and length about 7 km. [15, 16, 17, 18]. Asmari formation is consisted from three main reservoirs Jeribe Euphrates, Upper Kirkuk and Middle-Lower Kirkuk.

Jeribe Euphrates is the upper part of Asmari formation that deposited during Neogene geological period. In reservoir studies, it is indicated as A zone, have a lithology consists mainly of 85% dolomite alternated with moderately 15% thin shale and little anhydrate at its top, so dolomite is the main component of this part that derived from Tertiary reservoirs in southern Iraq. This reservoir has three subzones A1, A2 and A3., with average thickness 40 m [19, 20].

Upper Kirkuk Reservoir is a middle reservoir of Asmari formation, deposited during

Open Access
No. 40, September 2023, pp. 59-73

P- ISSN: 2220-5381
E- ISSN: 2710-1096

Paleogene geological period. It is denoted as B zone and consisting basically of thick shale, alternated with thin sandstone, Argillaceous limestone, and limestone. The sandstone component is gray, weakly consolidated, finer to moderate coarse, subangular to particular thread, slightly ordered, argillaceous bonded loose, and mainly silica. Local 5-35% faint yellow direct fluorescence, and moderately streaming milky white cut fluorescence. It has average thickness 120 m divided to four subzones B1, B3, B3 and B4. It is the best reservoir that contain the biggest amount of hydrocarbon reserves of Asmari formation due to existing sandstone with high porosity and permeability [15].

Middle-Lower Kirkuk Reservoir is a lower reservoir of Asmari formation that deposited along Paleogene geological epoch, Oligocene series and stage of Aquitanian to lower Oligocene. It is represented as C and D units, its lithology composed mainly from thick shale and argillaceous siltstone alternated with moderately thick argillaceous limestone and sandstone with average thickness 200 m. [15]. [21] on his study showed C zone as a part of Upper Kirkuk reservoir with title Buzurgan member, this difference of characterization due to evaluation diversity.

2. Material and Methods

Compressional sonic (*DTC*), density (*RHOB*), and gamma ray (*GR*) logs of three X3, X4, and XD wells that produced from Asmari reservoir at Y oil field are used for determination of P_p as shown in **Figure (3)**. X3, and X4 are vertical wells while XD is a directional well. X3 and XD wells located at north dome of Y field while X4 exists at south dome. These three wells had P_p measurement by modular dynamic tester *(MDT*) that used for calibration calculated values.

Open Access
No. 40, September 2023, pp. 59-73

P- ISSN: 2220-5381
E- ISSN: 2710-1096

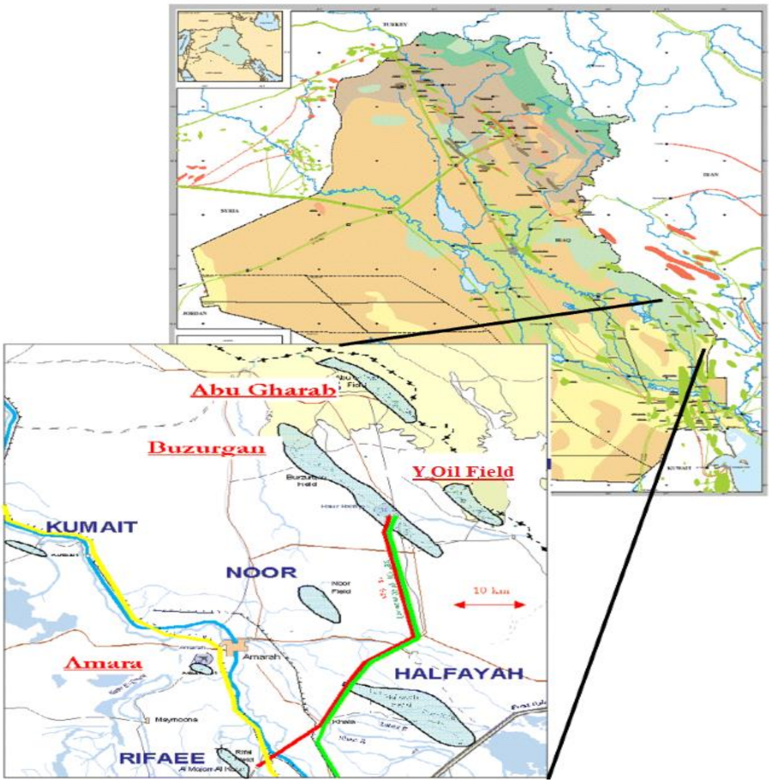

Fig. (2): Y oil field location on Iraq map [22].

Number of measured points of X3, X4, and XD wells are 22, 38, and 14 respectively at different depths. Asmari reservoir that had three main mention reservoirs are classified to multi subzones A zone belongs to Jeribe Euphrates reservoir, B1, B2, B3, and B4 zones correspond to Upper Kirkuk Reservoir, and C zone mention to Middle-Lower Kirkuk Reservoir. This classification is based on different in lithology and fluid contents.

The key component for pore pressure estimation is a vertical stress (S_v) [23]. It sometime called overburden pressure, or lithostatic pressure that represent the stress caused by an overlaying vertical column of rocks and fluids [24]. S_v increases with depth at rate around 20 MPa/km (often 0.8 to 1.0 psi/ft) [25]. *Sv* calculation is mainly depend on existing of bulk density. *RHOB* may be used to acquire the bulk density data [26] but it is not frequently measured for the shallow depths of a well, then, these shallow intervals density must be determined in order to calculate the total vertical stress.

In present study, density is linearly extrapolated with exiting density log to determine bulk density form zero depth to target formation depth by following equation [27]:

$$\rho_{EXT} = \rho_{MGL} + A_o.(TVD - AG - WD)^n \qquad (1)$$

Open Access
No. 40, September 2023, pp. 59-73

P- ISSN: 2220-5381
E- ISSN: 2710-1096

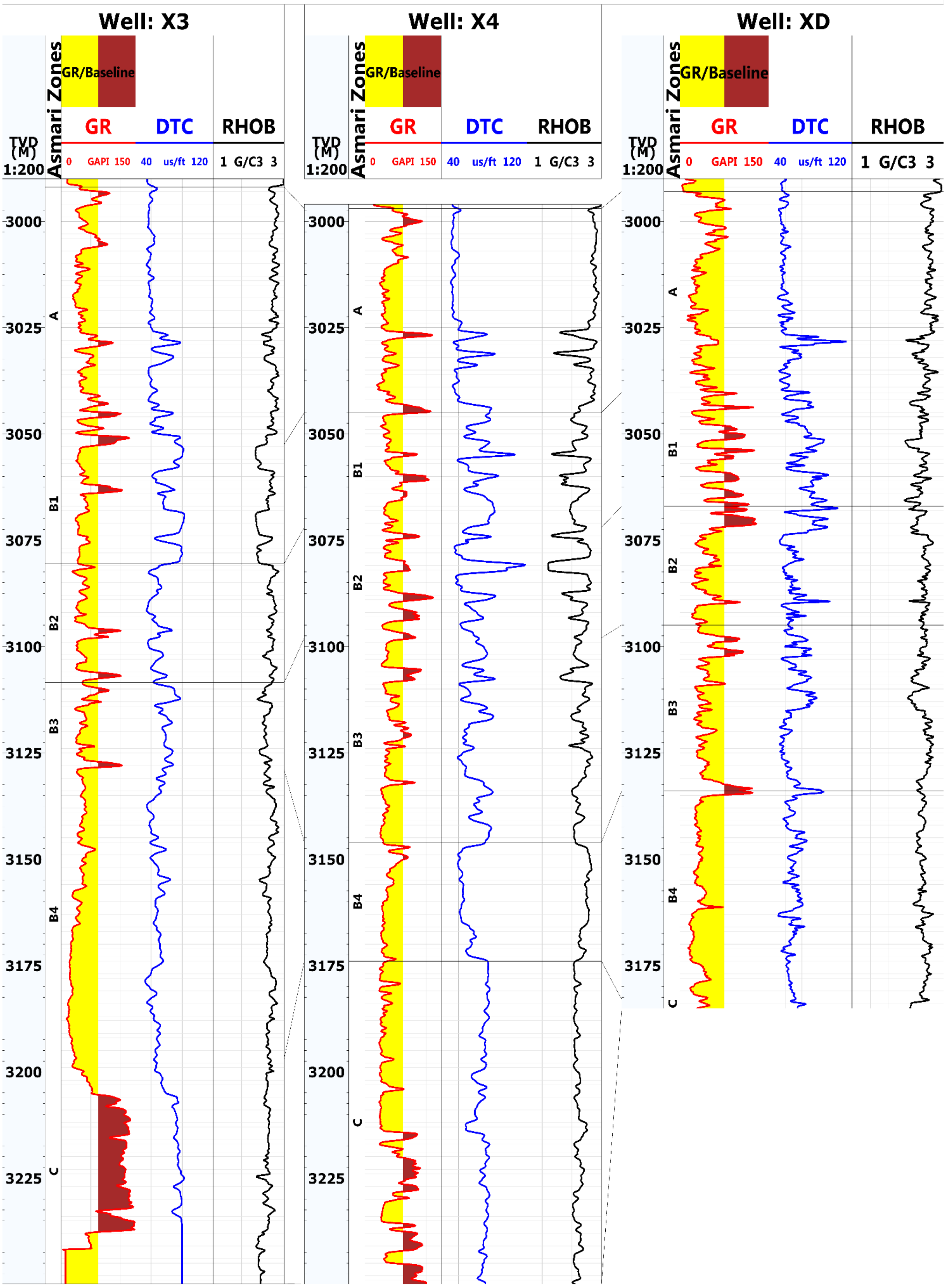

Fig. (3): Adopted logs X3, X4, and XD wells in present study.

Open Access
No. 40, September 2023, pp. 59-73

P- ISSN: 2220-5381
E- ISSN: 2710-1096

Where ρ_{EXT}, is calculated density for shallow depths by linear extrapolation (gm/cc), $\boldsymbol{\rho_{MGL}}$ is a sea floor or ground level density (gm/cc), *TVD* represent a true vertical depth (m), *AG* and *WD* are air gap and water levels from earth surface (m), and A_o and *n* are fitting parameters.

The extrapolated bulk density from the density log for a column of sediments, starting from the surface to the depth of interest, may be integrated as follows [28]:

$$S_v = \int_{D_w}^{D} \rho_{EXT}.g.D\,dD = \rho'_{EXT}.g.D \quad (2)$$

where ρ'_{EXT} (gm/cc) denotes the average density of overburden rocks at depth (*D*) (m or ft) respectively, and *g* (m or ft per s^2) denotes the earth's acceleration.

Pore pressure is firstly calculated as a P_{norm} by the following equation [3]:

$$P_{norm} = \rho_f.g.TVD \quad (3)$$

Where P_{norm} is the normal pore pressure in pounds per square inch (psi) and ρ_f is the fluid column density in grams per cubic centimeter (gm/cc).

Two methods are used for detecting over pressure intervals but that after determination of shale flags where must of over pressure zones is consisting from shale. Shale flag identification was based on gamma ray (*GR*) log with a threshold value of 75 *GAPI*.

Eaton method, one of the most used pore pressures estimating methods in the field, was developed as a result of Eaton's work in the Gulf of Mexico. The Eaton approach employs a normal compaction trend line that is semi-logarithmic. Resistivity, sonic, seismic interval velocity, or D-exponent are some of the different log measures that the Eaton method uses [28, 29]. For both seismic and sonic applications, Author of [30] is developed a modified Eaton approach. At zero effective stress, the modification makes up for the unphysical behavior as follow:

$$P_P = S_v - (S_v - P_{norm})\left(\frac{DTC_n}{DTC}\right)^x \quad (4)$$

Bowers (1995) examined the associated sonic interval velocities using well logging data from the Gulf of Mexico coast and estimated the effective stresses from the recorded pore pressure data of the shale and overburden stresses. Pore pressure was calculated using the effective stress component in the Terzaghi equation [31, 32]:

$$P_P = S_v - \left[\frac{10^6.(\frac{1}{DTC}-\frac{1}{DTC_n}}{A}\right]^{\frac{1}{B}} \quad (5)$$

Open Access
No. 40, September 2023, pp. 59-73

P- ISSN: 2220-5381
E- ISSN: 2710-1096

Where: *DTC* in (us/ft) in shale at P_{norm}, DTC_n is compressional sonic time (us/ft) in shale established from log. *x* is based on the trend line for typical compaction where equal to 3 [33], *A* and *B* are calibrated parameters equal to 4.457 and 0.8 respectively as default values.

3. Results and Discussion

Calculated S_v of three wells is presenting in **Figure (4)**. The results of S_v revealed that the gradient of the directional northern dome well (XD) is 1.03 psi/ft. Vertical wells (X3) located at the northern Y oil field dome exhibit a vertical stress gradient equal to 0.99 psi/ft, whereas the gradient of the vertical well (X4) in the south Y oil field dome is 0.93 psi/ft. When compared to theoretical values (0.8 - 1 psi/ft), these gradients are extremely acceptable. The gradient of the X4 well differs from that of the other wells because it is located in the south dome of the field, while the others are in the north dome.

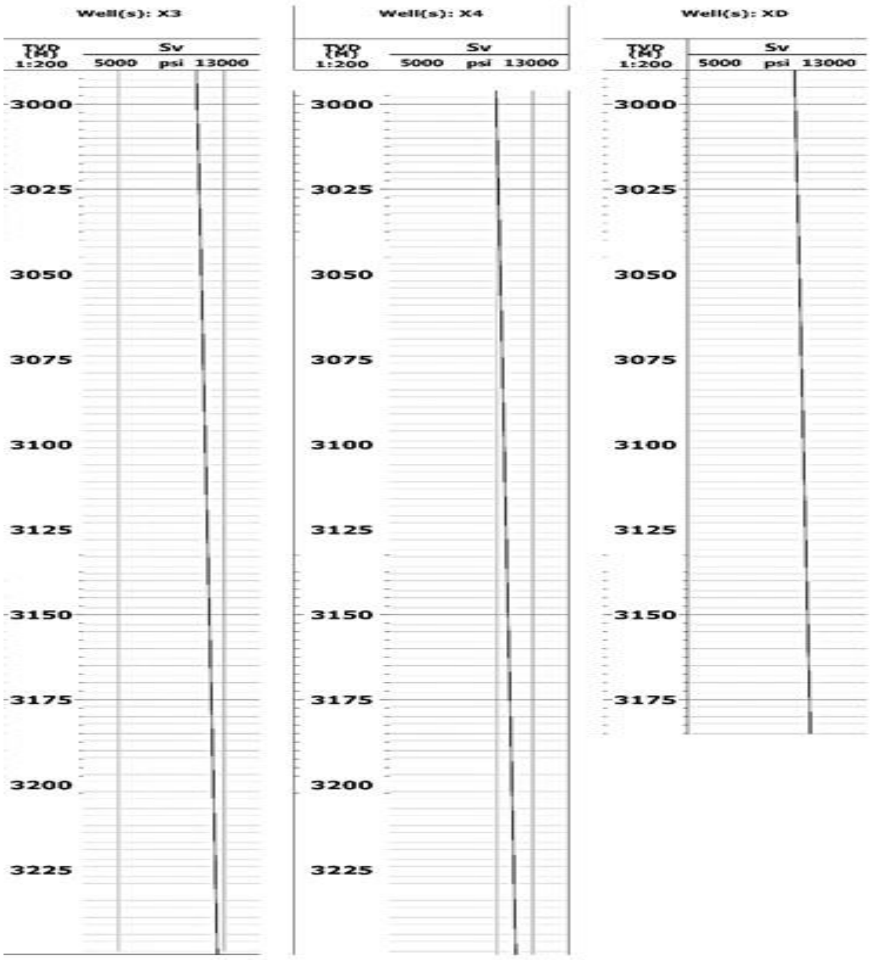

Fig. (4): Calculated verticals stress of X3, X4, and XD well.

Open Access
No. 40, September 2023, pp. 59-73

P- ISSN: 2220-5381
E- ISSN: 2710-1096

Estimated shale flag is depicted in **Figure (5)**. It is showed highly matching with lithology tracks and these depths are expecting to show over pore pressure.

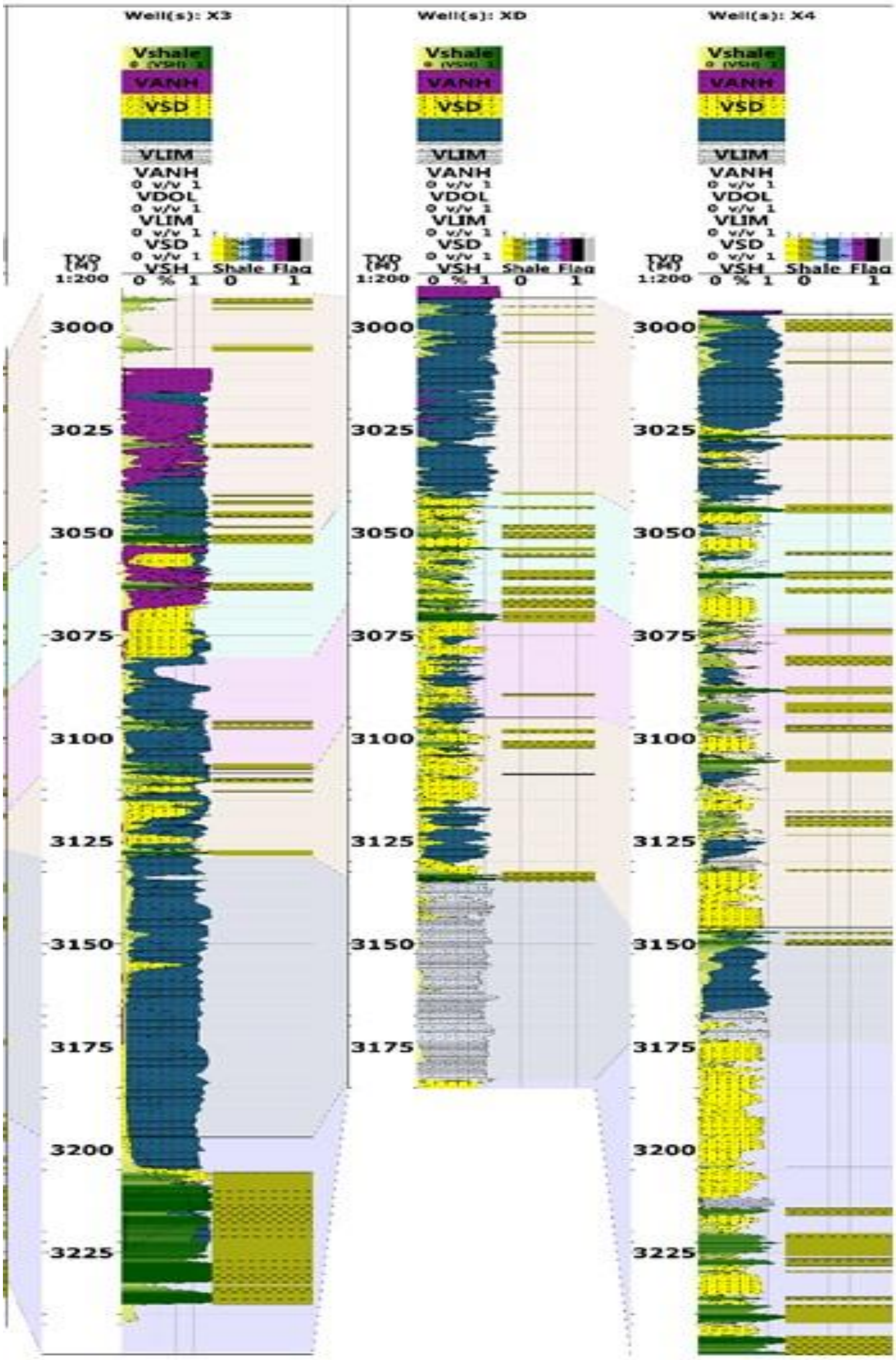

Fig. (5): Shale flag in three wells intervals.

Pore pressure is firstly calculated as a P_{norm} for all intervals by using **Eq. (3)**, but after determination of shale flags of three wells as shown in previous **Figure (5)**, Eaton slowness and Bowers original **Eqs. (4)** and **(5)** are used for calculating over (Abnormal) pressure of

Open Access
No. 40, September 2023, pp. 59-73

P- ISSN: 2220-5381
E- ISSN: 2710-1096

detected shale intervals. *MDT* measurements are used for calibration calculated P_p in two methods as shown in **Figure (6)**.

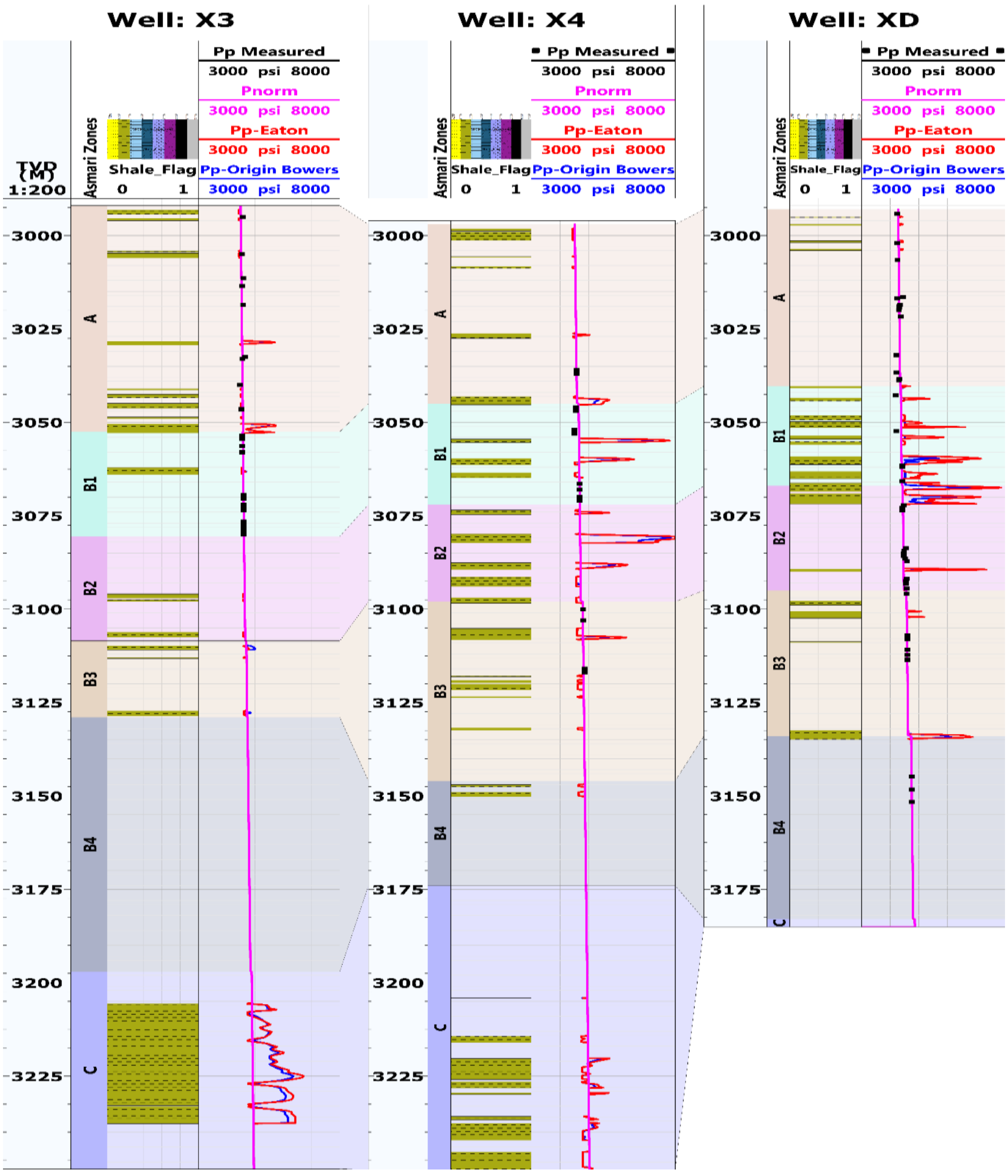

Fig. (6): Pore pressure calibration of three wells.

Bowers' original equation supplied abnormal pressure values of shale intervals better than Eaton's slowness equation since the latter didn't identify all shale intervals, when some shale *DTC* readings were low, and did not cut by *DTC* cutoff baseline that equaled (80 us/ft) in contrast provided very high values for other shale intervals, furthermore, changing of *x* parameter in ranges between 2.8 to 3.3 did not provide any matching with measured pore pressure, whereas Bowers original equation considers nearly all shales intervals by adjusting

Open Access
No. 40, September 2023, pp. 59-73

P- ISSN: 2220-5381
E- ISSN: 2710-1096

two parameters A and B values to produce the best match with *MDT* data. As a consequence, the adopted values are computed P_{norm} for clean intervals and pore pressure (P_p) taken from Bowers' original equation for shale intervals as abnormal pore pressure. Maximum percent error between predicted and measured pore pressure of wells (X3, X4, and XD) are 1.2%, 0.89% and 3% respectively where these percent's are very acceptable. **Table (1)** lists A and B parameters of Bower original **Eq. (5)** for all zones. Based on obtained results, average reservoir pressure of north dome zones is 4720 psi and for south dome is 4750 psi, these values are very closed with cited values in final well reports.

Table (1) Bowers original equation parameters for all zones wells.

Well Name	Zone	A	B
X3	A	4.4567	0.86
	B1	4.4567	0.858
	B2	4.4567	0.86
	B3	4.4567	0.86
	B4	4.4567	0.86
	C	4.4567	0.855
X4	A	4.4567	0.865
	B1	4.4567	0.865
	B2	4.4567	0.865
	B3	4.4567	0.86
	B4	4.4567	0.869
	C	4.4567	0.859
XD	A	4.4567	0.86
	B1	4.4567	0.845
	B2	4.4567	0.86
	B3	4.4567	0.86
	B4	4.4567	0.86
	C	4.4567	0.855

Maximum over pressure values in Asmari formation zones at wells are as follows: 6328 psi at depth 3225 m in well X3, 7538 psi at depth 3080 m in well X4, and 6731 psi at true vertical depth 3067 m in well XD. Over pressure values in two north dome wells are closed, whereas X4 well in south dome has a larger over pressure value than the rest. As a result, similar to these intervals in future wells will drill must considered in utilizing drilling fluids to avoid drilling problems.

4. Conclusions

Pore pressure estimation is very important parameter that must be determined before drilling a well or producing from wells. Over (Abnormal) pressure intervals are causing many problems

Open Access
No. 40, September 2023, pp. 59-73

P- ISSN: 2220-5381
E- ISSN: 2710-1096

during drilling so it must be detecting. Compressional and density logs of three X3, X4, and XD wells that located in Y oil field and producing from Asmari reservoir are used for estimation pore pressure. Vertical stress is calculated for these three wells by using extrapolated bulk density of density logs. Pore pressure is firstly predicted as normal pore pressure, while secondly is estimated by two methods of Eaton slowness and Bowers original after shale flags determination. Bowers original method was better than Eaton slowness in over (Abnormal) pore pressure intervals detection because the last did not cut all shale intervals by compressional sonic log shale base line. Changing of Eaton parameter (x) to different values did not affect largely on all calculated over pressure values because some of shale intervals had low *DTC* reading that did not cut by baseline. All detected high pressure intervals at six zones must be considering in future wells. Average reservoir pressure of north dome zones is 4720 psi and for south dome is 4750 psi, these values are very closed with cited values in final well reports. These values will provide driller an ideal about zones will face during drilling, so can be dealing it accurately.

Nomenclators

ρ_f = Fluid column density (gm/cc)

A and B = Calibrated parameters equal to 4.457 and 0.8 respectively as default values.

AG = Air gap level from earth surface (m).

A_o and n = Fitting parameters

D = Depth (m)

DTC = Compressional sonic log (us/ft)

DTC_n = Compressional sonic time in shale established from log (us/ft).

MDT = Modular dynamic tester

P_{norm} = Normal pore pressure (psi)

P_p = Pore pressure (psi)

RHOB = Density log (gm/cc)

Sv = Vertical stress (psi)

TVD = True vertical depth (m).

WD = Water level from earth surface (m)

x = Eaton equation parameter (default = 3)

ρ_{EXT}, = Calculated density for shallow depths by linear extrapolation (gm/cc).

ρ_{MGL} = Sea floor or ground level density (gm/cc).

Open Access
No. 40, September 2023, pp. 59-73

P- ISSN: 2220-5381
E- ISSN: 2710-1096

References

[1] S. Esmaeilpour, and I. Ispas, "Pore Pressure Prediction Using Model Based Seismic Inversion and Downhole Measurements," Paper presented at the 55th U.S. Rock Mechanics/Geomechanics Symposium, June 18–25, 2021. ARMA-2021-1584, 2021.

[2] R. I. Nwonodi, and A. Dosunmu, "A Geomodel for Pore Pressure Prediction Based on A Viscoelastic Compaction Law," Paper presented at the SPE Nigeria Annual International Conference and Exhibition, Lagos, Nigeria, August 2019. SPE-198730-MS, 2019. https://doi.org/10.2118/198730-MS.

[3] M. Elmahdy, A. E. Farag, E. Tarabees, and A. Bakr, "Pore Pressure Prediction in Unconventional Carbonate Reservoir," Paper presented at the SPE Kingdom of Saudi Arabia Annual Technical Symposium and Exhibition, Dammam, Saudi Arabia, SPE-194224-MS, 2018. https://doi.org/10.2118/194224-MS.

[4] A. Liaw, T. K. Kan, N. Kennedy, K. Belk, and. F. L. Gallice, "Integrated Pore Pressure Prediction in Gunnison Field," SEG/San Antonio, Annual Meeting, 2007.

[5] A. Mese, "Pore Pressure Effect on Mechanical and Acoustic Properties in Shale and Sand," Geomechanics E&R. SEG/Houston, Annual Meeting, 2005.

[6] G. V. Chillingar, V. A. Serebryakov, and J. O. Robertson, "Origin and Prediction of Abnormal Formation Pressures," Elsevier, 2002.

[7] B. Bruce, and G. Bowers, "Pore pressure terminology," The Leading Edge, 21(2), pp. 170–173, 2002. https://doi.org/10.1190/1.1452607.

[8] R. E. Swarbrick, and M. J. Osborne, "Mechanisms that generate abnormal pressures: an overview," American Association of Petroleum Geologists. Vol. 70, 1998. https://doi.org/10.1306/M70615.

[9] M. A. Gutierrez, N. R. Braunsdorf, and B. A. Couzens, "Calibration and ranking of pore-pressure prediction models," The leading Edge, 1516-1523, 2006. https://doi.org/10.1190/1.2405337.

[10] M. A. Issa, and F. A. Hadi, "Coupled Reservoir Geomechanics with Sand Production to Minimize the Sanding Risks in Zubair Oil Field", Petroleum Science and Technology, vol. 40, no. 9, pp. 1065-1083, 2021. https://doi.org/10.1080/10916466.2021.2014522

[11] H. Rabia, "Well Engineering and Construction Hussain Rabia," pp.1 to 789, 2002.

[12] D. P. Krynine, and W. R. Judd, "Principles of Engineering Geology and Geotechnics,"

Open Access
No. 40, September 2023, pp. 59-73

P- ISSN: 2220-5381
E- ISSN: 2710-1096

McGraw-Hill, New York, N.Y., 1957.

[13] S. S. Marsden, and S. N. Davis, "Geological subsidence," Sci. Am., 216: pp. 93-100. 1967. https://doi.org/10.1016/S0070-4571(08)70776-3.

[14] J. J. Zhang, "Applied Petroleum Geomechanics," Gulf Professional Publishing, Elsevier, United States, 2019.

[15] Q. A. Abdul-Aziz, and H. A. Abdul-Hussain, "Integration of Geomechanical and Petrophysical properties for estimating rate of penetration in Fauqi oil field Southern Iraqi," Doctorate dissertation, University of Baghdad, Collage of Engineering, Iraq, 2021.

[16] J. Mohammed Al Said Naji, G. H. Abdul-Majeed, and A. K. Alhuraishawy, "Comparison of Estimation Sonic Shear Wave Time Using Empirical Correlations and Artificial Neural Network", IJCPE, vol. 23, no. 4, pp. 49–58, Dec. 2022. https://doi.org/10.31699/IJCPE.2022.4.7

[17] J. M. Al Said Naji, G. H. Abdul-Majeed, and A. K. Alhuraishawy, "Intelligent Approach for Investigating Reservoir Heterogeneity Effect on Sonic Shear Wave", Journal of Petroleum Research and Studies, vol. 13, no. 1, pp. 56-73, Mar. 2023. https://doi.org/10.52716/jprs.v13i1.680

[18] J. M. Al Said Naji, G. H. Abdul-Majeed, A. K. Alhuraishawy, and A. R. Abbas, "Prediction of Sanding Likelihood Intervals Using Different Approaches", Journal of Petroleum Research and Studies, vol. 13, no. 2, pp. 1-15, Jun. 2023. https://doi.org/10.52716/jprs.v13i2.698

[19] W. I. Taher, M. S. Al Jawad and C. W. V. Kirk, "Reservoir study for Asmari reservoir/Fauqi field," Master thesis, University of Baghdad, Collage of Engineering, Iraq, 2011.

[20] J. M. Al Said Naji, G. H. Abdul-Majeed, and A. K. Alhuraishawy, "Prediction of Sonic Shear Wave using Artificial Neural Network," paper accepted by Iraqi Journal Geological Journal, 2022. https://doi.org/10.46717/igj.55.2E.10ms-2022-11-24

[21] B. A. Al-Baldawi, "Building A 3D Geological Model Using Petrel Software for Asmari Reservoir, South Eastern Iraq", Iraqi Journal of Science, vol. 56, no. 2C, pp. 1750–1762, Apr. 2023. https://ijs.uobaghdad.edu.iq/index.php/eijs/article/view/10026.

[22] A. H. S. Al-Ekabi, "Erratum to: Microfacies and environmental study of the Mishrif Formation in Noor Field," Arab J Geosci, vol.8, pp. 5795–5808, 2015. https://doi.org/10.1007/s12517-015-1784-9

Open Access
No. 40, September 2023, pp. 59-73

P- ISSN: 2220-5381
E- ISSN: 2710-1096

[23] B. Amadei, and O. Stephansson, "Rock stress and its measurement," Springer, Berlin, 1997.

[24] A. Ranjbar, H. Hassani, and K. Shahriar, "3D geomechanical modeling and estimating the compaction and subsidence of Fahlian reservoir formation (X-field in SW of Iran)", Arabian Journal of Geosciences, 10, Article number: 116, 2017. https://doi.org/10.1007/s12517-017-2906-3

[25] S. Ashooria, M. Abddidehb, and M. T. Hayavic, "Prediction of critical flow rate for preventing sand production using the Mogi-Coulomb failure criterion," Journal of Social Sciences (Lahore), 26(5), pp. 2029-2032, 2014. http://www.sci-int.com/pdf/5590518521%20a--2029-2032-Ashoori-IRAN.pdf.

[26] Z. Bassiouni, "Theory, measurement, and interpretation of well logs," vol 4. Henry L. Doherty Memorial Fund of AIME, Society of Petroleum Engineers, 1994.

[27] Schlumberger Service Company, "Techlog Software Manual," 2018.

[28] B. A. Eaton, "The equation for geopressure prediction from well logs," Paper presented at the Fall Meeting of the Society of Petroleum Engineers of AIME, SPE-5544-MS, 1975. https://doi.org/10.2118/5544-MS.

[29] B. A. Eaton, "The Effect of Overburden Stress on Geopressure Prediction from Well Logs," J Pet Technol 24 (08): pp. 929–934. SPE-3719-PA, 1972. https://doi.org/10.2118/3719-PA.

[30] K. Katahara, "Analysis of Overpressure on the Gulf of Mexico Shelf," Paper presented at the Offshore Technology Conference, Houston, Texas, OTC-15293-MS, 2003. https://doi.org/10.4043/15293-MS.

[31] G. Bowers, "Pore Pressure Estimation from Velocity Data: Accounting for Overpressure Mechanisms Besides Under compaction," SPE Drill & Compl 10 (02): pp. 89–95, 1995. SPE-27488-PA. https://doi.org/10.2118/27488-PA.

[32] J. Zhang, "Pore pressure prediction from well logs: Methods, modifications, and new approaches," Earth-Science Reviews. Vol. 108, pp 50–63, 2011. https://doi.org/10.1016/j.earscirev.2011.06.001.

[33] M. Azadpour, and S. N. Manaman, "Determination of pore pressure from sonic log: a case study on one of Iran carbonate reservoir rocks," Iranian Journal of Oil and Gas Science and Technology, 4(3), pp. 37-50, 2015.